Superposing compass states for asymptotic isotropic sub-Planck phase-space sensitivity

Atharva Shukla [1,2] and Barry C. Sanders [1]

[1]*Institute for Quantum Science and Technology, University of Calgary, Alberta, Canada T2N 1N4*
[2]*Department of Physics, Indian Institute of Technology Roorkee, Uttarakhand-247667, India*

Compass states deliver a sub-Planck phase-space structure in the sense that sensitivity to phase-space displacement is superior to the sensitivity of displacing the vacuum state in any direction, but this sensitivity is anisotropic: better sensitivity for some directions of phase-space displacement versus others. Here we introduce generalized compass states as superpositions of n compass states, with each oriented by $\pi/2n$ with respect to its predecessor. Specifically, we derive Wigner functions for these generalized compass states and approximate closed-form expressions for overlaps between generalized compass states and their displaced counterparts. Furthermore, we show that generalized compass states, in the limit $n \to \infty$, display isotropic sensitivity to phase-space displacement in any direction.

I. INTRODUCTION

Historically, the coherent state was introduced first by Schrödinger [1] and subsequently, in seminal work for quantum optics by Glauber [2]. The coherent state, being a displaced vacuum state, captures the essence of the position-momentum uncertainty relation ($\Delta x \Delta p \geqslant \hbar/2$) derived from $[\hat{a}, \hat{a}^\dagger] = \mathbb{1}$ for $\hat{a}$ the annihilation operator with $\hat{x} = \hat{a} + \hat{a}^\dagger$ and $i\hat{p} = \hat{a} - \hat{a}^\dagger$ the position and momentum operators, respectively. Inspired by Schrödinger's cat-state argument about philosophical implications of quantum mechanics [1], a quantum optics version of a cat state [3], known at first as even and odd coherent states [4], was shown to deliver displacement sensitivity superior to what can be achieved for the coherent state [5–8]; this displacement sensitivity technically means that displacing the state in phase space [9], i.e., applying some combination of position and momentum displacements, yields a smaller overlap than is achieved by applying the same displacement to a coherent state.

Zurek introduced the compass state, which is a superposition of four coherent states rotated by $\pi/2$ relative to each predecessor, which can be pictured as a superposition of coherent states in the north, south, east, and west of phase space relative to the origin. Then Zurek showed that displacing such a state in any direction of phase space is more sensitive in *every* direction than for the initial coherent state (placed anywhere in phase space) [5], and this compass state was later connected to physical implementations [10,11] and Heisenberg-limited measurements [7]. Zurek's analysis shows that the sub-Planck phase-space sensitivity delivered by the compass state has relevant applications in setting limits on the sensitivity of quantum meters and in accelerated decoherence. In a compass state, the size of the smallest perturbation that makes the displaced state approximately orthogonal and hence distinguishable from the original state is far beyond the "standard quantum limit." These results also make it possible to anticipate the mesh structure required to simulate a quantum system's evolution in phase space.

We note that this compass state has been generalized to other group symmetries [12,13], but here we generalize in a different way: we superpose compass states at various orientations and show that, asymptotically for infinitely many such compass states superposed, such a generalized compass state has sub-Planck phase-space displacement sensitivity that is isotropic with respect to phase-space direction. This phase-space isotropicity delivers equal sub-Planck resolution regardless of which linear combination of canonical position x and position p is being measured. This isotropicity is absent for a single compass state where a perturbation in some phase-space direction might make the displaced state approximately orthogonal and hence distinguishable from the original state while not having the same effect when applied in some other phase-space direction. Our superposition of compass states could be especially useful in the context of quantum metrology.

There have been multiple proposals and realisations of sub-Planck phase-space structures. These include the use of dispersive interaction between atoms and a high-quality cavity [10,11]. Apart from this, there have been multiple actual experimental implementations [14–18] and their properties have been studied in different contexts [6,19–30].

In Sec. II we present salient notions and the notation we use. We introduced some compact notation, which is quite helpful for us to keeping concepts clear. Then we present the results in Sec. IV. We discuss our results in Sec. V and present our conclusions and outlook in Sec. VI.

II. CONCEPTS AND NOTATION

Now we discuss the concepts and our notation for cat states and compass states and their generalization. We begin with the coherent state and the cat state as a superposition of two coherent states, and then proceed to discuss and introduce notation for compass states, which are superpositions of two cat states and generalized compass states. We connect compass

states and generalized compass states, which are superpositions of compass states, to the concept of superpositions of coherent states on a circle in phase space [31]. Finally, we discuss Wigner functions as representations of such states and simplified versions that capture essential features and ignore relatively minor features.

Mathematically, the coherent state is

$$|\alpha\rangle := D(\alpha)|0\rangle, \quad \alpha \in \mathbb{C}, \tag{1}$$

where

$$D(\alpha) := \exp\{\alpha\hat{a}^\dagger - \text{H.c.}\} \tag{2}$$

is the Glauber-Sudarshan displacement operator, $|0\rangle$ the vacuum state, and H.c. denotes the Hermitian conjugate [32]. For simplicity, we introduce the notation $|a\rangle$ for $a \in \mathbb{R}^+$ as we only require a positive real-valued coherent state for our purposes. The even and odd cat state is then

$$|a\rangle_\pm := |a\rangle \pm |-a\rangle, \tag{3}$$

and all our states are implicitly normalized so we do not write explicitly the normalization coefficients. For convenience we represent the even cat state by $|{-}\rangle := |a\rangle_+$, with the amplitude a suppressed because the amplitude a is fixed to be the same for all states discussed herein.

Now we show how to extend an even cat state to a compass state and superpositions thereof. The $\pi/2$-rotated version of an even coherent state is expressed simply as

$$||\rangle := R(\pi/2)|{-}\rangle, \quad R(\theta) := e^{i\theta\hat{a}^\dagger\hat{a}}. \tag{4}$$

We denote the compass state by

$$|\Diamond\rangle = ||\rangle + |{-}\rangle, \tag{5}$$

which is a special case of coherent states on the circle [31,33]. Furthermore, we introduce the convenient rotated-state notation

$$| \rangle_\theta := R(\theta)| \rangle \Rightarrow |\alpha\rangle = |a \equiv |\alpha|\rangle_{\arg \alpha}. \tag{6}$$

Thus,

$$|\Diamond\rangle_\theta := R(\theta)|\Diamond\rangle, \tag{7}$$

with special cases

$$|\Diamond\rangle_{\pi/4} := |\square\rangle, \quad |\Diamond\rangle_{\pi/6} := |\square\rangle, \quad |\Diamond\rangle_{\pi/3} := |\square\rangle. \tag{8}$$

A superposition of n compass states rotated by a fixed amount with respect to the predecessor and equidistributed over phases from 0 to 2π is

$$\sum_{m=0}^{n-1} |\Diamond\rangle_{m\pi/2n}, \tag{9}$$

which is a special case of superpositions of coherent states on a circle in phase space, which has been studied in quite general form but not specifically for the restricted case (9) here [31].

Wigner functions $W(x, p)$ are representations of states that help us to visualize quantum states as phase-space representations [9]. Wigner functions are a close quantum analog of classical phase-space distributions [9,34]. For a pure state $|\psi\rangle$,

$$W(x, p; \psi) := \int_{\mathbb{R}} dy\, e^{ipy/\hbar} \psi^*(x + y/2)\psi(x - y/2), \tag{10}$$

which is not explicitly normalized per our convention. As a special case, the Wigner function for the coherent state $|a\rangle$ (1) is

$$W_\bullet(x, p; a) = \exp\{-[p^2 + (x - 2a)^2]/2\}, \tag{11}$$

where $\bullet$ denotes a coherent state in our short-hand notation. The Wigner function for the cat state $|{-}\rangle$ is

$$W_-(x, p; a) = W_\bullet(x, p; a) + W_\bullet(x, p; -a) \\ + 2e^{-(x^2+p^2)/2}\cos(2ap), \tag{12}$$

with the subscript $-$ denoting the even cat state. This cat-state Wigner function (12) is the sum of Wigner functions for two coherent states (11) along with a third "interference" term.

Now we introduce notation and expressions for the superposition of four coherent states in two cases using the north-south-east-west language explained in Sec. I: the north-south case and the east-west case.

First, we introduce Wigner functions for the Gaussian lobes of the cat states. Specifically, the Wigner function

$$W_:(x, p; a) := W_\bullet(p, x; a) + W_\bullet(p, x; -a) \tag{13}$$

with $:$ our short-hand notation to denote the two coherent states at the north and south ends of the compass, which does not include the interference terms between them. The next term is

$$W_{..}(x, p; a) := W_\bullet(x, p; a) + W_\bullet(x, p; -a) \tag{14}$$

with $..$ our notation for two coherent states at the east and west points of the compass and without interference terms.

Now we introduce the remaining terms required to write the Wigner function of a compass state. First, we use the notation

$$W_+(x, p; a) := 2e^{-(p^2+x^2)/2}[\cos(2ap) + \cos(2ax)], \tag{15}$$

for the interference pattern at the center. This Wigner function is calculated according to the contribution of the interference terms from the two cat states formed by the diagonally opposite coherent states. Next, we consider interference terms for adjacent cat states in the northwest, northeast, southwest, and southeast directions and write

$$W_\Diamond := 2 \sum_{\sigma_x, \sigma_p = \pm 1} G(\sigma_x x, \sigma_p p), \tag{16}$$

with $\Diamond$ being our notation to represent the rhombus and

$$G(x, p; a) := e^{-1/2((x-a)^2 + (p-a)^2)} \times \cos[a(x + p - a)]. \tag{17}$$

Combining all these terms yields the full Wigner function

$$W_\Diamond = W_: + W_{..} + W_\Diamond + W_+ \tag{18}$$

for the entire compass state. The Wigner function for rotated compass states (8) can be found similarly by rotating the coordinate system. Now we define sensitivity to displacement in phase space and Planck scale.

Definition 1 (Sensitivity). For any given small real-valued threshold, the sensitivity of the state is the smallest magnitude of displacement over all phase-space directions such that the overlap of the displaced state with the original state is less than the threshold.
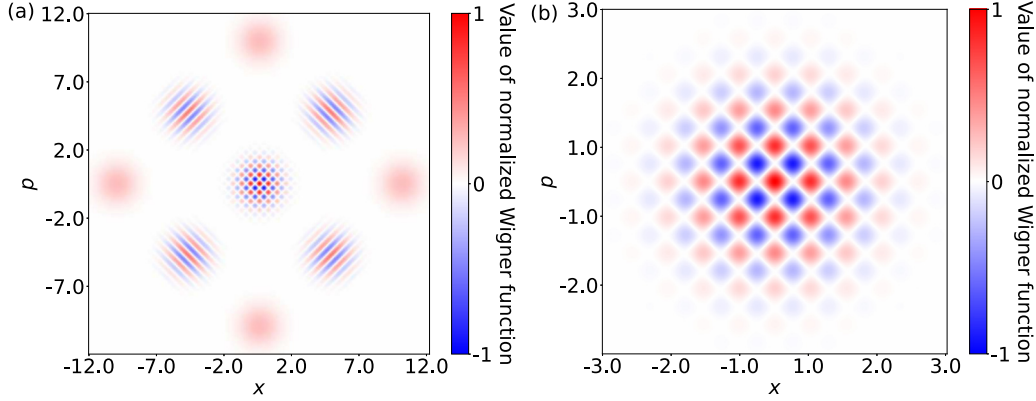
FIG. 1. Heat map for the normalized Wigner function of a compass state with $a = 5$ (a) shown fully and (b) the center interference pattern only.

Now we explain phase-space displacement and how it can be used to quantify sensitivity and establish the Planck scale.

To quantify the sensitivity of phase-space displacement on a state, we employ the overlap between a state and its δ-displaced version, namely,

$$\gamma(\delta; |\psi\rangle) := |\langle\psi||D(\delta)||\psi\rangle|^2 \Rightarrow \gamma(0; |\psi\rangle) = 1 \forall |\psi\rangle. \quad (19)$$

If $\gamma(\delta; |\psi\rangle) = 0$, the orthogonality condition

$$|\psi\rangle \perp D(\delta)|\psi\rangle \quad (20)$$

holds and thus the two states in Eq. (20) are perfectly distinguishable. Sensitivity does not require that the overlap be zero, but rather only needs to be small enough with respect to a small real-valued threshold ϵ. Thus, sensitivity is quantified by $|\delta|_{\min}$, which is given by $|\delta|$ satisfying

$$\min_{|\delta|, \arg\delta} \gamma(\delta; |\psi\rangle) < \epsilon, \quad (21)$$

with respect to the given threshold ϵ. Thus, we employ $|\delta|_{\min}$ as the sensitivity quantifier in accordance with Definition 1.

We quantify the sensitivity of the state $|\psi\rangle$ to displacement by calculating the smallest $|\delta|$ such that the orthogonality condition (20) holds. Smaller $|\delta|_{\min}$ such that Eq. (20) holds indicates a more sensitive state. For the study of the sensitivity of superpositions of compass states, the expression

$$\begin{aligned}
{}_{\theta_1}\langle a|D(\delta)|a'\rangle_{\theta_2} &= \exp\{-i(a\sin\theta_1(a'\cos\theta_2 + \mathrm{Re}(\delta)))\} \\
&\times \exp\{-i(-a\cos\theta_1(a'\sin\theta_2 + \mathrm{Im}(\delta)))\} \\
&\times e^{i(\mathrm{Im}(\delta)a'\cos\theta_2 - \mathrm{Re}(\delta)a'\sin\theta_2)} e^{-|ae^{i\theta_1} - a'e^{i\theta_2} - \delta|^2/2}
\end{aligned}$$

$$(22)$$

is handy later. The simple version

$$_{\theta}\langle a|D(\delta)|a\rangle_{\theta} = e^{2i(a\mathrm{Im}(\delta)\cos\theta - a\mathrm{Re}(\delta)\sin\theta) - |\delta|^2/2}, \quad (23)$$

holds for

$$a = a', \quad \theta_1 = \theta_2 \quad (24)$$

with the squared magnitude being

$$|\langle a|D(\delta)|a\rangle|^2 = e^{-|\delta|^2}. \quad (25)$$

Importantly, the right-hand side of Eq. (25) is independent of the choice of coherent state. Now that we established the

concepts and notation for compass states, we proceed to study the properties of compass states and its superpositions.

III. BACKGROUND ON THE COMPASS STATE

In this section, we review the properties of a compass state $|\diamondsuit\rangle$ as knowledge of these properties is vital for our contributions in subsequent sections. We begin by reporting the Wigner function (10) for the compass state and the overlap of a compass state with its displaced counterpart. Finally, we report the solution for the phase-space regions where this overlap function is approximately zero.

We present a plot of the Wigner function for the compass state in Fig. 1(a). The full expression is discussed in Sec. II. We choose $a = 5$, i.e., five times the Planck scale in phase space, because this choice of a effectively suppresses the overlap between coherent states (whose size is given by a) and nearest neighbors. In this case, the observed phase-space interference arises for distinct coherent states. Choosing small a for the compass state would be analogous to forming kitten, rather than cat, states, corresponding to superpositions of overlapping coherent states [35]. We choose a such that the distance between the adjacent coherent states of our state is at least six standard deviations, i.e., six units.

The smallest interference structures arise from coherence between pairs of coherent states maximally separated by angle in phase space, i.e., up to π, available to them in the phase space [5]. The linearity of interference means that we do not need to treat interference between all coherent states but rather between pairs; note that this approach leads to a factorially growing number of pairwise interference terms so we also have a strategy for reducing an $n!$ cost to a cost of $2n$ with n the number of compass states, each with four coherent states superposed. As we are only concerned with the center part of phase space, where sensitivity is the highest, we focus on the interference term near the center.

Now we explain technically how we calculate the Wigner function for the center of phase space for a single compass state. A compass state has four equally spaced coherent states on the circle in the north (N), south (S), east (E), and west (W) of phase space as introduced in Sec. I. There are $\binom{4}{2}$ cat states in the compass state. The interference pattern near the center is formed by the contribution of only the pairs of coherent
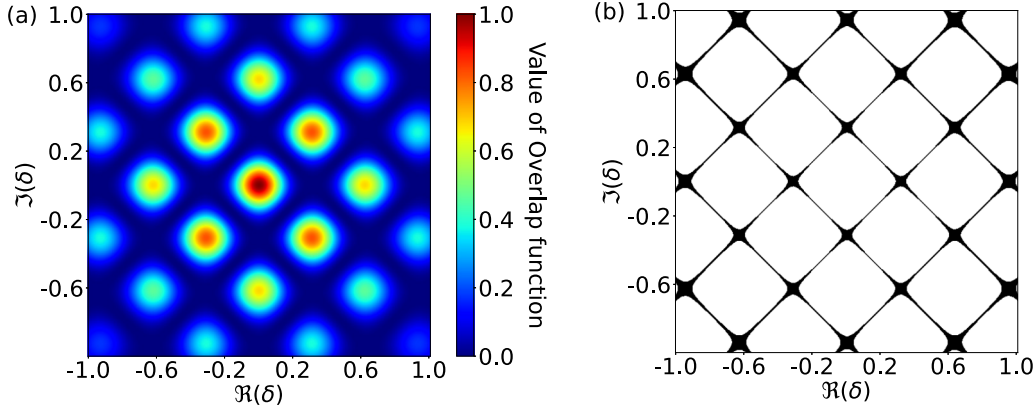
FIG. 2. Heat map for the overlap function of a compass state with $a = 5$ (a) shown fully and (b) the phase-space regions where its value is approximately zero.

states maximally separated by angle in phase space (π), i.e., from the interference of the N-S and E-W pairs of coherent states. We ignore the contributions from the interference of the N-E, E-S, S-W, and W-N cat states. The Wigner-function representation is

$$W_+(x, p) = 2e^{-1/2(x^2+p^2)}[\cos(2xa) + \cos(2pa)]. \quad (26)$$

This is a sign-alternating pattern; the area of the tile of this chessboard-like pattern is equal to $\pi^2/2a^2$. As the area is proportional to a^{-2}, it is smaller than $\hbar^2$ for $a \gg 1$, which corresponds to sub-Planck structures [5].

A similar alternating chessboard pattern emerges for a mixture of a horizontal and vertical cat state as well. However, sensitivity is enhanced only for certain phase-space directions [12], which casts some doubt over the importance of the sub-Planck phase-space structure as a way to assess enhanced sensitivity. Phase-space displacement sensitivity avoids this problem [5].

To determine the phase-space displacement sensitivity of a compass state, we need to calculate an approximation of the overlap of a compass state with its displaced counterpart. The full expression for the compass state is complicated, and previous work presents the overlap function for a simplified case that ignores cross terms, corresponding to superpositions of some pairs of coherent states, with this neglect of cross terms not explicitly stated [12]. Here we calculate the full exact expression (B1) as we need to consider cross terms carefully in superposing compass states.

We now explain the method for ignoring negligible cross terms using the following terminology: the original compass state as a superposition of north, south, east, and west coherent states in phase space with the displaced compass state comprising a superposition of coherent states at positions north′, south′, east′, and west′. The neglected cross terms correspond to the following:

(1) north-south′ (NS′), north-east′ (NE′), north-west′ (NW′);

(2) south-north′ (SN′), south-east′ (SE′), south-west′ (SW′);

(3) east-north′ (EN′), east-west′ (EW′), east-south′ (ES′);

(4) west-north′ (WN′), west-east′ (WE′) and west-south′ (WS′)

cases, which contribute negligibly to phase-space displacement sensitivity for sufficiently large a. As a increases, we can see that the cross terms vanish from our derivation of the exact expression (B1). The approximate overlap for a compass state with its δ-displaced self is

$$\gamma(\delta; \diamondsuit) \approx e^{-|\delta|^2} |\cos[2a\,\mathrm{Im}(\delta)] + \cos[2a\,\mathrm{Re}(\delta)]|^2 \quad (27)$$

neglecting the cross terms.

Now we depict the approximate insensitivity of γ (27) to the direction of displacement δ in phase space. In Fig. 2 we present a plot of γ (27) versus δ and the regions where γ is approximately zero (< 0.001). As seen in Fig. 2(b), the region of phase space where γ is close to zero encloses the origin. The origin signifies the overlap with the unperturbed state, i.e., perfect overlap,

$$\gamma(0; |\diamondsuit\rangle) = 1, \quad (28)$$

which holds for the exact version of γ (B1) as well. Furthermore, for displacement direction $\arg(\delta)$ in phase space, $\gamma = 0$ has infinitely many periodic solutions, with the period depending on the direction of displacement.

Now we proceed to calculate the smallest $|\delta|$ for which γ (27) vanishes to quantify the sensitivity given by Eq. (21) of the compass state, which corresponds to solving

$$\cos[2a\,\mathrm{Im}(\delta)] + \cos[2a\,\mathrm{Re}(\delta)] = 0, \quad (29)$$

whose solutions are

$$\mathrm{Im}(\delta) \pm \mathrm{Re}(\delta) = {}^{(2m+1)\pi}/_{2a}, \ m \in \mathbb{Z}. \quad (30)$$

The minimum magnitude of displacement is thus

$$|\delta|_{\min} = {}^{\pi}/_{2\sqrt{2}a}, \quad \arg\delta = {}^{(2m+1)\pi}/_4, \quad m \in \{0, 1, 2, 3\}, \quad (31)$$

with the four solutions corresponding to the four coherent states superposed to make a compass state. Our aim in superposing compass states is to devise a state for which the sensitivity is approximately constant over all $\arg(\delta) \in [0, 2\pi)$.

IV. RESULTS

In this section, we study the specific case of the superposition of two compass states in Sec. IV A. We calculate the Wigner function and solutions for the phase-space regions
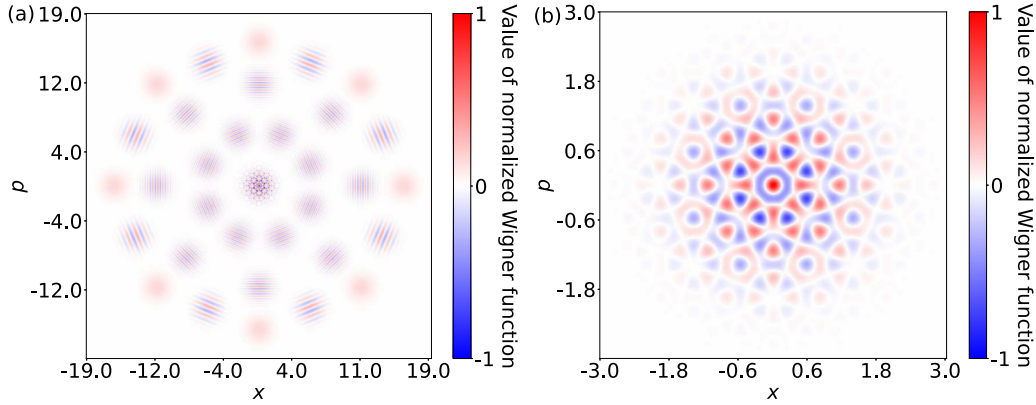
FIG. 3. Heat map for the normalized Wigner function of the superposition of two compass states with $a = 8$ (a) shown fully and (b) the center interference pattern only.

where $\gamma \approx 0$. Subsequently, we generalize our results for an arbitrary number n of compass states in Sec. IV B.

A. Superposition of two compass states

Now we consider a superposition of just two compass states, continuing our approach of not explicitly normalizing states in mathematical expressions, but regarding states as implicitly normalized. We only consider superpositions of compass states comprising superpositions of coherent states with equal magnitudes of displacement from the origin, i.e., states of the type $|\diamondsuit\rangle_\theta$ (7). For our purposes, only their mutual separation matters. Furthermore, we restrict to a superpostion of two compass states with mutual rotation $\pi/4$, namely,

$$|\diamondsuit\rangle + |\square\rangle \qquad (32)$$

using the unnormalized-state convention discussed just below Eq. (3). We present in this subsection the Wigner function for this state and then the overlap function γ.

We present a plot of the Wigner function for the superposition of two compass states (32) in Fig. 3. These plots can be compared to the Wigner function plots for a single compass state in Fig. 1. The Wigner function consists of a number of rings. The outermost ring corresponds to the coherent states part of our compass states and the interference of the cat state formed by the adjacent coherent states. The next inner ring comprises the interference terms of the cat states formed by alternating coherent states. Following the same pattern, the inner-most ring is the superposition of interference of cat states formed by opposite coherent states. At the center of the Wigner function, the smallest phase-space structures are found.

In the present case of a superposition of two compass states, we have

$$\binom{8}{2} = 28 \qquad (33)$$

cat states. To calculate the center interference of the Wigner function, we only consider the cat states formed by the pairs of coherent states maximally separated by angle in phase space as in Sec. III. The Wigner function, due to the interference at

the center, is

$$W_{\text{cent}}(x, p) \approx 2e^{-1/2(x^2+p^2)}[\cos(2xa) + \cos(2pa)$$
$$+ \cos(\sqrt{2}(pa + xa)) + \cos(\sqrt{2}(pa - xa))]. \qquad (34)$$

For simplicity, we have only to consider the central interference pattern shown in Fig. 3(b), as the smallest phase-space structures are at the center, making the central interference pattern the most relevant.

For the superposition of two compass states, we can label coherent states on the circle in phase space by the compass coordinates

$$\text{N, NE, E, SE, S, SW, W, NW,} \qquad (35)$$

with NE denoting northeast and so on. Similarly, we write N′ and so on for coordinates of the eight coherent states of the displaced superposition of two compass states. The cross terms are denoted by NE-SW′ and so on. As we have eight coherent states, and the cross terms do not include self-terms such as N-N′, $7 \times 8 = 56$ cross terms exist. We do not consider any of these 56 terms; only the eight self-terms

$$\text{N-N}', \text{ S-S}', \text{ E-E}', \text{ W-W}', \text{ NE-NE}', \text{ SW-SW}',$$
$$\text{NW-NW}', \text{ SE-SE}' \qquad (36)$$

are nonnegligible. Calculating the overlap as in Sec. III, we obtain

$$\gamma(\delta; |\diamondsuit\rangle + |\square\rangle) \approx e^{-|\delta|^2} \left| \sum_{m=0}^{1} \{\cos[2a|\delta| \cos(\arg\delta + {}^{m\pi}/4)] \right.$$
$$\left. + \cos[2a|\delta| \sin(\arg\delta + {}^{m\pi}/4)]\} \right|^2, \qquad (37)$$

which has a period $\pi/4$ over $\arg\delta$.

We plot γ (37) versus δ and the regions where $\gamma \approx 0$ by setting a numerical cutoff of

$$\gamma < 0.001 \qquad (38)$$

in Fig. 4. This cutoff is not the threshold ϵ (39), but rather a round-off that ensures sufficiently sharp lines in Fig. 4. The region of phase space where $\gamma \approx 0$ encloses the origin. The
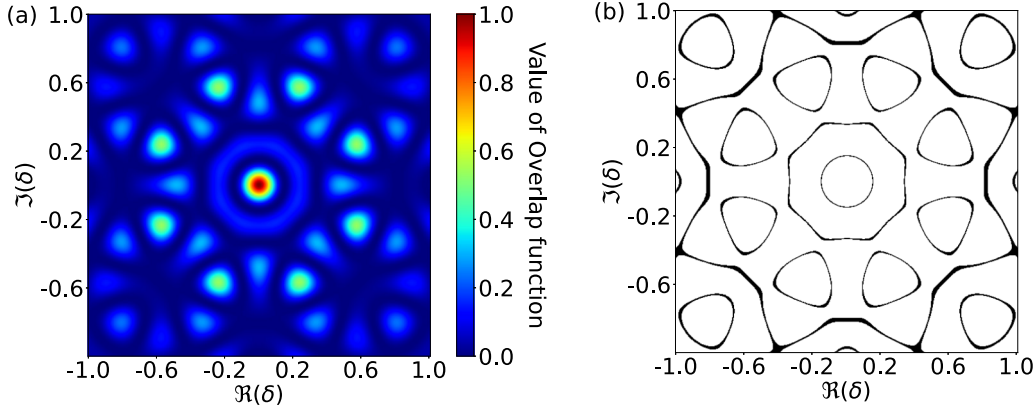
FIG. 4. Heat map for the overlap function of the superposition of two compass states with $a = 8$ (a) shown fully and (b) the phase-space regions where its value is approximately zero.

overlap between the superposition of two compass states and their displaced version goes to zero for any arbitrary direction of displacement. Now we determine the regions in phase space such that the overlap γ is less than the threshold

$$\epsilon \leftarrow 10^{-15}, \tag{39}$$

i.e., assigned the value 10^{-15}. We solve for the roots of Eq. (37), namely,

$$\sum_{m=0}^{1} \{\cos[2a|\delta| \cos(\arg\delta + {}^{m\pi}/_4)]$$
$$+ \cos[2a|\delta| \sin(\arg\delta + {}^{m\pi}/_4)]\} \equiv 0, \tag{40}$$

which is an exact equality but leads only to an approximation of γ as shown in Eq. (37). This expression identifies all δ such that $\gamma(\delta; |\diamondsuit\rangle + |\square\rangle)$ vanishes.

To obtain approximate solutions, we assign the direction of phase-space displacement as $\arg\delta$ and assign the size a pertaining to both compass states in the superposition. We then calculate the Taylor series for Eq. (40) around some $y \in \mathbb{R}$. Truncating the Taylor series to quadratic order introduces a change of the order of 10^{-9} in the values of $|\delta|$ for which $\gamma < \epsilon$. This truncation is valid because the error due to Taylor series truncation is orders of magnitude smaller than ϵ.

Now that we know this truncation is valid, we can neglect cubic and higher-order terms in the expansion, which yields a quadratic expression. Thus, a good approximation for γ is given by the quadratic equation characterized by the coefficients A_2 (D1), B_2 (D2), and C_2 (D3) in the quadratic equation

$$A_2|\delta|^2 + B_2|\delta| + C_2 = 0, \tag{41}$$

as elaborated in Sec. D. The $_2$ in the coefficients' subscripts (41) indicates the number of compass states n in our superposition. These coefficients can be simplified using the Jacobi-Anger expansion (D4) to obtain the ultimate expressions for coefficients A_2, B_2, and C_2 of in Eq. (41).

The coefficients (41) are valid for the region

$$||\delta| - y| \ll 1, \tag{42}$$

i.e., satisfying the Taylor series truncation approximation, and the direction of phase-space displacement $\arg\delta$. For $J_n(z)$ the

nth Bessel function of the first kind, these coefficients are

$$A_2(y; a, \arg\delta) = 4a^2[J_2(2ay) - J_0(2ay)]$$
$$+ 2a^2 \cos(8\arg\delta)[2J_6(2ay)$$
$$+ 2J_{10}(2ay) - 4J_8(2ay)] \tag{43}$$

for the quadratic term

$$B_2(y; a, \arg\delta) = -2A_2y - 8aJ_1(2ay)$$
$$+ 8a\cos(8\arg\delta)[J_7(2ay) - J_9(2ay)] \tag{44}$$

for the linear term, and

$$C_2(y; a, \arg\delta) = -A_2y - B_2 + 4J_0(2ay)$$
$$+ 8\cos(8\arg\delta)[J_8(2ay)] \tag{45}$$

for the constant. All three coefficients have small oscillations with period ${}^{\pi}/_4$ over $\arg\delta$. The roots of Eq. (41) are

$$|\delta| = \frac{-B_2 \pm \sqrt{B_2^2 - 4A_2C_2}}{2A_2}. \tag{46}$$

The roots are the magnitude of displacement $|\delta|$ for which γ vanishes in a specific direction of phase-space displacement $\arg\delta$.

We now quantify the sensitivity of this state, given by Definition 1, for the arbitrary case. We solve for the roots of Eq. (41), and the resultant coefficients are given by Eqs. (43) to (45).

In the neighborhood of $y = {}^6/_{5a}$, the roots oscillate in the region

$$\frac{1}{a}[1.20223545, 1.20259051], \tag{47}$$

with period ${}^{\pi}/_4$ over the direction of displacement $\arg\delta$. The sensitivity of the state is quantified by

$$|\delta|_{\min} = {}^{1.20223545}/_a, \tag{48}$$

which is obtained for

$$\arg\delta = {}^{(2m+1)\pi}/_8. \tag{49}$$

As $|\delta|_{\min}$ greatly exceeds the Planck scale for $a \gg 1$, this superposition of two compass states delivers substantial sub-Planck resolution in phase space.

Next, we generalize these results for the case of the superposition of n compass states.

B. Generalized superposition

We are now in a position to generalize the results to a superposition of n compass states, each of size a and each rotated by an angle

$$m\pi/2n, \quad m \in \{0, 1, 2, \ldots, n-1\}. \tag{50}$$

Our superposition is thus

$$\sum_{m=0}^{n-1} |\diamondsuit\rangle_{m\pi/2n}. \tag{51}$$

As before, we calculate the center interference part of the Wigner function. Then we calculate the overlap function for this general case. Finally, we solve the roots for this overlap to determine the sensitivity of this superposition of an arbitrary number of compass states.

In the present case of a superposition of n compass states, we have

$$\binom{4n}{2} = \frac{4n(4n-1)}{2} \tag{52}$$

cat states. To calculate the center interference of the Wigner function, we only consider the cat states formed by the pairs of coherent states maximally separated by angle, i.e., by π radians, in phase space, as done in the previous sections.

The Wigner function, due to the interference at the center, is

$$
W_{\mathrm{cen}}(x, p) \approx 2e^{-1/2(x^2+p^2)} \sum_{m=0}^{n-1} \left\{ \cos\left[2xa\sin\left(\frac{m\pi}{2n}\right)\right. \right.
$$
$$
\left. - 2ap\cos\left(\frac{m\pi}{2n}\right)\right] + \cos\left[2ax\sin\left(\frac{m\pi}{2n}\right)\right.
$$
$$
\left. \left. + 2ap\cos\left(\frac{m\pi}{2n}\right)\right]\right\}. \tag{53}
$$

We see a Gaussian envelope as the coefficient for this expression. This envelope modulates a sum of functions, and these functions are cosines of a sum of cosine and sine functions

For special values of n, Eq. (53) reduces to our previous Eqs. (26) and (34). The general expression for the Wigner function of the center interference pattern is given by Eq. (53).

We follow the process outlined in the previous sections to neglect cross terms in the overlap. As we have $4n$ coherent states, and the cross terms do not include self-terms such as N-N', only $4n(4n-1)$ cross terms remain. We neglect these terms so only the self-terms are nonnegligible. Calculating the overlap, we obtain

$$
\gamma\left(\delta; \sum_{m=0}^{n-1} |\diamondsuit\rangle_{\frac{m\pi}{2n}}\right)
$$
$$
\approx e^{-|\delta|^2} \left| \sum_{m=0}^{n-1} \left\{ \cos\left[2a|\delta|\cos\left(\arg\delta + \frac{m\pi}{2n}\right)\right] \right. \right.
$$
$$
\left. \left. + \cos\left[2a|\delta|\sin\left(\arg\delta + \frac{m\pi}{2n}\right)\right]\right\}\right|^2, \tag{54}
$$

with a Gaussian coefficient in terms of $|\delta|^2$ and a sum of cosine functions of sinusoidal functions. Furthermore, γ exhibits a period of $\pi/2n$ over $\arg\delta$ for n compass states. We can see that Eq. (54) reduces to the special cases of Eqs. (27) and (37) when $n \in \{1, 2\}$, respectively. We solve for the roots of Eq. (54), namely,

$$
\sum_{m=0}^{n-1} \{\cos[2a|\delta|\cos(\arg\delta + m\pi/2n)]
$$
$$
+ \cos[2a|\delta|\sin(\arg\delta + m\pi/2n)]\} \equiv 0, \tag{55}
$$

which is an exact equality but leads only to an approximation of γ as shown in Eq. (54). Similar to our previous cases, we truncate the Taylor series to quadratic order to calculate Eqs. (F1) to (F3). As shown in Appendix F these equations can be further simplified using Eq. (D4) to obtain the coefficients A_n, B_n, and C_n. The expressions for these coefficients are

$$
A_n(y; a, \arg\delta) = 2a^2 n[J_2(2ay) - J_0(2ay)]
$$
$$
+ na^2 \cos(4n\arg\delta)[2J_{4n-2}(2ay)
$$
$$
+ 2J_{4n+2}(2ay) - 4J_{4n}(2ay)] \tag{56}
$$

for the quadratic term

$$
B_n(y; a, \arg\delta) = -2A_n y - 4anJ_1(2ay) + 4an\cos(4n\arg\delta)
$$
$$
\times [J_{4n-1}(2ay) - J_{4n+1}(2ay)] \tag{57}
$$

for the linear term, and

$$
C_n(y; a, \arg\delta) = -A_n y^2 - B_n y + 2nJ_0(2ay)
$$
$$
+ 4n\cos(4n\arg\delta)[J_{4n}(2ay)] \tag{58}
$$

for the constant. For the special case of superposition of two compass states ($n = 2$), Eqs. (56) to (58) reduce to Eqs. (43) to (45).

Upon increasing the number n of compass states, the isotropic nature of the superposition of compass state increases because, as $n \to \infty$, the Bessel function of the first kind

$$
J_n(y) = \sum_{l=0}^{\infty} \frac{(-1)^l y^{2l+n}}{2^{2l+n}l!(n+l)!} \tag{59}
$$

tends to zero. Hence, the oscillatory part for all three coefficients in Eqs. (56) to (58) vanishes. Due to this, the quadratic equation remains the same for all directions of phase-space displacements. The state thus has uniform sensitivity.

V. DISCUSSION

Now we give a high-level summary of our results. To recap, we solved for cases of superpositions of a few compass states: the trivial yet enlightening case of one compass state (to clarify the issues in the previous literature), and superpositions of two compass states. Then we generalize to the case of a superposition of any finite number of compass states.

In each case, we plot the exact Wigner function and a blown-up version of the center of the exact Wigner function. We see these plots for one compass state in Fig. 1, for the superposition of two compass states in Fig. 3.

In all the cases, we approximate the analytical expression for the center interference. We recognize that only the cat states formed by opposite coherent states significantly contribute to our center interference pattern. The analytical expressions only consider these terms. This approximation reduces the number of terms significantly as the total terms grow combinatorially with the number of compass states in our superposition. The plots of center interference are blown-up versions of our plots of the whole Wigner function.

In all the cases, we calculate the approximate analytical expressions for the overlap functions. We neglect all cross terms that vanish exponentially for increasing a, which previously was implied but not stated explicitly [12]. We plot these approximate overlap functions and the regions where the overlap function is approximately equal to 0 for one compass state in Fig. 2 and for the superposition of two compass states in Fig. 4. The overlap functions are periodic in all cases.

The innermost rings in Figs. 2 and 4 define the sensitivity. The magnitude of the smallest displacement from the origin to a point on this ring is the sensitivity of our state. As the number of compass states increases, the innermost ring becomes more isotropic in nature; i.e., the magnitude of the oscillations of the ring decreases. This increasing isotropicity can be seen by comparing the case of two compass states and the superposition of three compass states. The range of oscillation for the periodic inner ring in the case of the superposition of two compass states for an arbitrary value of a is $[^{1.20223545}/a, {}^{1.20259051}/a]$. For the superposition of three compass states this range reduces to $[^{1.202412739}/a, {}^{1.202412805}/a]$. The minimum of this range determines the sensitivity of our superposition. For any superposition, the sensitivity increases as a increases.

VI. CONCLUSION

In conclusion, we studied extensively the superpositions of compass states, motivated by extending Zurek's concept of sub-Planck phase-space displacement sensitivity in all directions of phase space [5] to delivering near-isotropic sub-Planck sensitivity to displacement. The study of sub-Planck phase-space sensitivity is important in setting the limits of quantum meters and anticipating the mesh structure required to simulate a quantum system's evolution. This near-isotropic feature delivers a robustness to "sub-Planckness" by not being subject to changes of the phase (weighting of the linear combination of canonical position and momentum). We attain the ideal case of near-isotropic sensitivity in all phase-space displacement directions as the number of compass states in the superposition becomes infinite. This ensures that a perturbation does not favor any phase-space direction. A perturbation on such a state will either make the displaced state approximately orthogonal to the original, irrespective of the phase-space direction or will not do so in any direction.

We note that the superposition of infinitely many compass states is also a superposition of infinitely many coherent states on a circle in phase space, which was studied as a basis for representations of any oscillator state [31]. However, our superpositions of an arbitrarily large number of compass states is not a special case of any cases or considerations in that seminal work as their focus on constructing an overcomplete basis focused on designing the phases of coherent states in the superposition. By analyzing superpositions of compass states rather than this more general case, near-isotropic sub-Planckness in phase space is clearer and even intuitive although, as we have shown, the mathematics is somewhat complicated.

Future work could consider experimental realizations of superpositions of compass states. Experimental realizations of a compass state have been explored [14–16], and an experimental realization could follow in that vein. These superpositions of compass states could have an impact on ultra-sensitive quantum metrology and efficient storage of quantum information, similar to the suggested impact of one compass state alone.

APPENDIX A: SUPERPOSITION OF THREE COMPASS STATES

Now we consider a superposition of just three compass states, continuing our approach of not explicitly normalizing states in mathematical expressions but regarding states as implicitly normalized. Similar to the case of the superposition of two compass states, we consider coherent states with equal magnitudes a of displacement from the origin in our superposition. We restrict to a superposition of three compass states with mutual rotation $\pi/6$, namely,

$$|\square\rangle + |\diamondsuit\rangle + |\diamondsuit\rangle,$$

$$|\diamondsuit\rangle := |\square\rangle_{30°}, \quad |\diamondsuit\rangle := |\square\rangle_{60°}. \quad (A1)$$

We present in this subsection the Wigner function for this state and then the overlap function γ.

Now we calculate and plot the Wigner function for the superposition of three compass states (A1) using approximations similar to those in Sec. IV A. Specifically, we plot the entire and exact Wigner function. Then we explain how we approximate the center interference pattern for the Wigner function.

The Wigner function is similar to the previous case of the superposition of two compass states and consists of multiple rings. These rings correspond to different interference terms of the cat states formed by the constituent coherent states of our compasses as we explained before.

Now we focus on the center interference pattern Fig. (5(b)). In the present case of a superposition of three compass states, we have

$$\binom{12}{2} = 66 \quad (A2)$$

cat states. To calculate the center interference of the Wigner function, we only consider the cat states formed by the pairs of coherent states maximally separated by angle, i.e., π radians, in phase space as in Sec. III. The Wigner function at the center
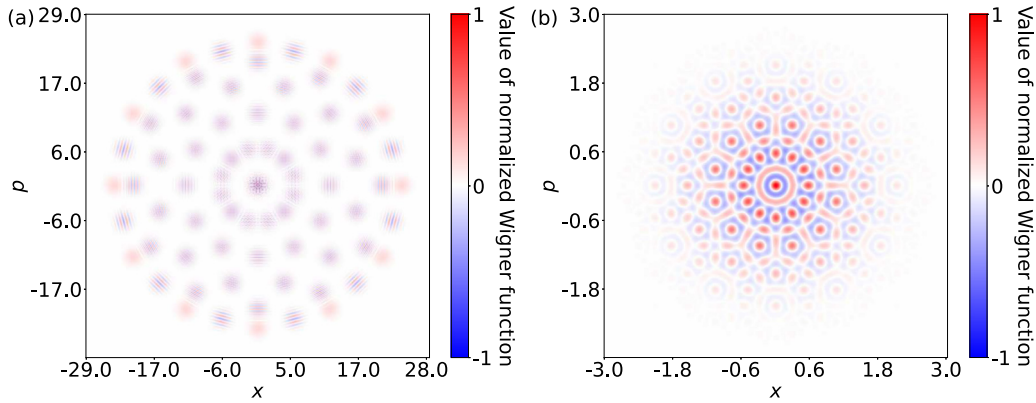
FIG. 5. Heat map for the normalized Wigner function of the superposition of three compass states with $a = 12$ (a) shown fully and (b) the center interference pattern only.

is

$$W_{\text{cen}}(x, p) \approx 2e^{-1/2(x^2+p^2)}[\cos(2xa) + \cos(2pa)$$
$$+ \cos(\sqrt{3}xa + pa) + \cos(\sqrt{3}pa - xa)$$
$$+ \cos(\sqrt{3}pa + xa) + \cos(\sqrt{3}xa - pa)] \quad \text{(A3)}$$

from six maximally separated pairs of coherent states (cats). Next, we focus on the overlap function. We follow the process outlined in Sec. IV A to neglect the cross terms in the overlap. As we have 12 coherent states, i.e., four coherent states per compass state and three compass states, and, as the cross terms do not include self-terms such as N-N′, precisely $11 \times 12 = 132$ cross terms exist. We do not consider any of these 132 terms; only the 12 self-terms are nonnegligible. Calculating the overlap as in Sec. III, we obtain

$$\gamma(\delta; |\square\rangle + |\diamondsuit\rangle + |\diamondsuit\rangle)$$

$$\approx e^{-|\delta|^2} \left| \sum_{m=0}^{2} \{\cos[2a|\delta| \cos(\arg\delta + {}^{m\pi}/_6)] \right.$$

$$\left. + \cos[2a|\delta| \sin(\arg\delta + {}^{m\pi}/_6)]\} \right|^2, \quad \text{(A4)}$$

which has a period of ${}^{\pi}/_6$ over $\arg \delta$.
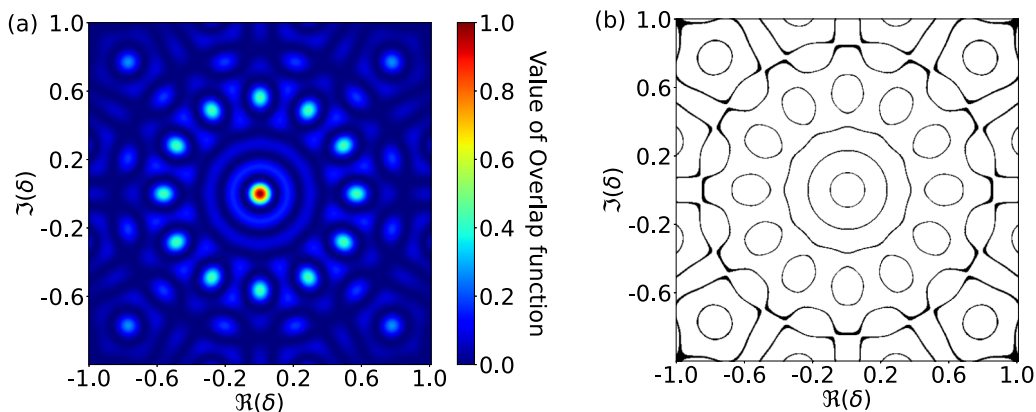
We plot γ (A4) vesus δ and the regions where $\gamma \approx 0$ by setting a numerical cutoff of $\gamma < 0.001$ in Fig. 6. This cutoff is not the threshold ϵ. The overlap between the superposition of three compass states and its displaced version goes to zero for any arbitrary direction of displacement.

Now we determine the regions in phase space such that the overlap γ is less than the threshold ϵ, which we set as 10^{-15} [39]. We solve for the roots of Eq. (A4), namely,

$$\sum_{m=0}^{2} \{\cos[2a|\delta| \cos(\arg\delta + {}^{m\pi}/_6)]$$

$$+ \cos[2a|\delta| \sin(\arg\delta + {}^{m\pi}/_6)]\} \equiv 0, \quad \text{(A5)}$$

which is an exact equality but leads only to an approximation of γ as shown in Eq. (A4). Equation (A5) identifies all δ such that

$$\gamma(\delta; |\square\rangle + |\diamondsuit\rangle + |\diamondsuit\rangle) \quad \text{(A6)}$$

vanishes.

We follow the process outlined in Sec. IV A and truncate the Taylor series to quadratic order. This introduces a change of the order of 10^{-9} in the values of $|\delta|$ for which $\gamma < \epsilon$.

FIG. 6. Heat map for the overlap function of the superposition of three compass states with $a = 12$ (a) shown fully and (b) the phase-space regions where its value is approximately zero.

The final expressions for the coefficients of the quadratic equation

$$A_3(|\delta|)^2 + B_3(|\delta|) + C_3 = 0 \tag{A7}$$

for a fixed $\arg \delta$ and a for the region (42) are

$$
\begin{aligned}
&A_3(y; a, \arg \delta) \\
&= 6a^2[J_2(2ay) - J_0(2ay)] + 3a^2 \cos(12 \arg \delta) \\
&\quad \times [2J_{10}(2ay) + 2J_{14}(2ay) - 4J_{12}(2ay)]
\end{aligned} \tag{A8}
$$

for the quadratic term,

$$
\begin{aligned}
B_3(y; a, \arg \delta) = &- 2A_3 y - 12aJ_1(2ay) + 12a \cos(12 \arg \delta) \\
&\times [J_{11}(2ay) - J_{13}(2ay)]
\end{aligned} \tag{A9}
$$

for the linear term, and

$$
\begin{aligned}
C_3(y; a, \arg \delta) = &- A_3 y - B_3 + 6J_0(2ay) \\
&+ 12 \cos(12 \arg \delta)[J_{12}(2ay)]
\end{aligned} \tag{A10}
$$

for the constant. Each coefficient comprises a constant and an oscillatory term similar to the case of the superposition of two compass states. The oscillations are periodic with period $\pi/6$ over $\arg \delta$. The roots of Eq. (A7) are

$$|\delta| = \frac{-B_3 \pm \sqrt{B_3^2 - 4A_3 C_3}}{2A_3}, \tag{A11}$$

with an angular period of $\pi/6$ evident in Fig. 6(b)

We now quantify the sensitivity of this state, given by Definition 1 for the arbitrary case when the size pertaining to the three compass states of our superposition is a. We solve the roots of Eq. (A7) characterized by Eqs. (A8) to (A10) for different values of $\arg \delta$.

In the neighborhood of $y = 6/5a$, the roots oscillate in the region

$$\frac{1}{a}[1.202412739, 1.202412805], \tag{A12}$$

with period $\pi/6$ over the direction of displacement $\arg \delta$. The sensitivity of the state is quantified by

$$|\delta|_{\min} = \frac{1.202412739}{a}, \tag{A13}$$

which is obtained for

$$\arg \delta = \frac{(2m + 1)\pi}{12}. \tag{A14}$$

The amplitude of oscillation has reduced when compared with the case of the superposition of two compass states; i.e., the isotropicity has increased with respect to the superposition of two compass states.

APPENDIX B: EXACT OVERLAP FUNCTION OF ONE COMPASS STATE

In this Appendix, we provide the exact overlap for the case of one compass state. In the following expression, we also consider the cross terms. These cross terms correspond to the following:

(1) north-south′ (NS′), north-east′ (NE′), north-west′ (NW′);
(2) south-north′ (SN′), south-east′ (SE′), south-west′ (SW′);
(3) east-north′ (EN′), east-west′ (EW′), east-south′ (ES′);
(4) west-north′ (WN′), west-east′ (WE′) and west-south′ (WS′)

cases. The exact expression is given by

$$
\begin{aligned}
|\langle \diamondsuit | D(\delta) | \diamondsuit \rangle|^2 = &|2e^{-|\delta|^2/2} \cos[2a\text{Im}(\delta)] + 2e^{-|\delta|^2/2} \cos[2a\text{Re}(\delta)] + e^{-|2a-\delta|^2/2} + e^{i[a\text{Im}(\delta)-a\text{Re}(\delta)+a^2]-|a-ia-\delta|^2/2} \\
&+ e^{i[a\text{Im}(\delta)+a\text{Re}(\delta)-a^2]-|a+ia-\delta|^2/2} + e^{i[-a\text{Im}(\delta)-a\text{Re}(\delta)-a^2]-|-a-ia-\delta|^2/2} + e^{i[-a\text{Im}(\delta)+a\text{Re}(\delta)+a^2]-|-a+ia-\delta|^2/2} \\
&+ e^{i[a\text{Im}(\delta)-a\text{Re}(\delta)-a^2]-|a+ia-\delta|^2/2} + e^{i[-a\text{Im}(\delta)-a\text{Re}(\delta)+a^2]-|a+ia-\delta|^2/2} + e^{i[a\text{Im}(\delta)+a\text{Re}(\delta)+a^2]-|-a-ia-\delta|^2/2} \\
&+ e^{i[-a\text{Im}(\delta)+a\text{Re}(\delta)-a^2]-|a-ia-\delta|^2/2} + e^{-|-2a-\delta|^2/2} + e^{-|-2ia-\delta|^2/2} + e^{-|-2ia-\delta|^2/2}|^2.
\end{aligned} \tag{B1}
$$

Making the radius of the circle, on which the coherent states are placed, significantly larger than Planck scale $a = 1$ makes the cross terms vanish exponentially.

APPENDIX C: DETAILS OF TAYLOR SERIES EXPANSION FOR THE SUPERPOSITON OF TWO COMPASS STATES

For the specific case of the superposition of two compass states, the overlap (37) vanishes when

$$\sum_{m=0}^{1} \{\cos[2a|\delta| \cos(\arg \delta + m\pi/4)] + \cos[2a|\delta| \sin(\arg \delta + m\pi/4)]\} \equiv 0. \tag{C1}$$

To obtain approximate solutions, we assign the direction of phase-space displacement as $\arg \delta$ and assign the size a pertaining to both compass states in the superposition. We then calculate the Taylor series for Eq. (C1) around some $y \in \mathbb{R}$. We truncate the Taylor series to quadratic order. The Taylor series of the first term in Eq. (C1) is

$$
\begin{aligned}
\cos[2a|\delta| \cos(\arg \delta + m\pi/4)] = &\cos[2ay \cos(\arg \delta + m\pi/4)] - \sin[2ay \cos(\arg \delta + m\pi/4)]2a \cos(\arg \delta + m\pi/4)(|\delta| - y) \\
&- \cos[2ay \cos(\arg \delta + m\pi/4)]2a^2 \cos^2(\arg \delta + m\pi/4)(|\delta| - y)^2
\end{aligned} \tag{C2}
$$

and the Taylor series of the second term in Eq. (C1) is

$$\cos[2a|\delta|\sin(\arg\delta + m\pi/4)] = \cos[2ay\sin(\arg\delta + m\pi/4)] - \sin[2ay\sin(\arg\delta + m\pi/4)]2a\sin(\arg\delta + m\pi/4)(|\delta| - y)$$
$$- \cos[2ay\sin(\arg\delta + m\pi/4)]2a^2\sin^2(\arg\delta + m\pi/4)(|\delta| - y)^2. \tag{C3}$$

The Taylor series of Eq. (C1) is the sum of both these series.

APPENDIX D: FORM OF QUADRATIC COEFFICIENTS FOR THE SUPERPOSITION OF TWO COMPASS STATES

The coefficients of the quadratic equation $[A_2(|\delta|)^2 + B_2(|\delta|) + C_2]$ for a fixed $\arg\delta$ and a for the region $||\delta| - y| \ll 1$ are

$$A_2(y; a, \arg\delta) = \sum_{m=0}^{1}\{-2a^2\sin^2(\arg\delta + m\pi/4)\cos[2ay\sin(\arg\delta + m\pi/4)]$$
$$- 2a^2\cos^2(\arg\delta + m\pi/4)\cos[2ay\cos(\arg\delta + m\pi/4)]\} \tag{D1}$$

for the quadratic term,

$$B_2(y; a, \arg\delta) = \sum_{m=0}^{1}\{4a^2y\sin^2(\arg\delta + m\pi/4)\cos[2ay\sin(\arg\delta + m\pi/4)] - 2a\sin(\arg\delta + m\pi/4)\sin[2ay\sin(\arg\delta + m\pi/4)]$$
$$+ 4a^2y\cos^2(\arg\delta + m\pi/4)\cos[2ay\cos(\arg\delta + m\pi/4)] - 2a\cos(\arg\delta + m\pi/4)\sin[2ay\cos(\arg\delta + m\pi/4)]\} \tag{D2}$$

for the linear term, and

$$C_2(y; a, \arg\delta) = \sum_{m=0}^{1}\{2ay\sin(\arg\delta + m\pi/4)\sin[2ay\sin(\arg\delta + m\pi/4)] - 2a^2y^2\sin^2(\arg\delta + m\pi/4)\cos[2ay\sin(\arg\delta + m\pi/4)]$$
$$+ \cos[2ay\sin(\arg\delta + m\pi/4)] + \cos[2ay\cos(\arg\delta + m\pi/4)] + 2ay\cos(\arg\delta + m\pi/4)\sin[2ay\cos(\arg\delta + m\pi/4)]$$
$$- 2a^2y^2\cos^2(\arg\delta + m\pi/4)\cos[2ay\cos(\arg\delta + m\pi/4)]\}. \tag{D3}$$

for the constant. We can simplify these to obtain Eqs. (43) to (45) using the Jacobi-Anger expansions of $\cos(z\cos\theta)$, $\cos(z\sin\theta)$, $\sin(z\sin\theta)$, and $\sin(z\cos\theta)$ given by

$$\cos(z\cos\theta) = J_0(z) + 2\sum_{n=1}^{\infty}(-1)^n J_{2n}(z)\cos(2n\theta),$$

$$\cos(z\sin\theta) = J_0(z) + 2\sum_{n=1}^{\infty}J_{2n}(z)\cos(2n\theta),$$

$$\sin(z\sin\theta) = 2\sum_{n=1}^{\infty}J_{2n-1}(z)\sin[(2n-1)\theta],$$

$$\sin(z\cos\theta) = -2\sum_{n=1}^{\infty}(-1)^n J_{2n-1}(z)\cos[(2n-1)\theta]. \tag{D4}$$

We further simplify Eq. (D1) to

$$A_2(y; a, \arg\delta) = \sum_{m=0}^{1}\{-2a^2\sin^2(\arg\delta + m\pi/4)\cos[2ay\sin(\arg\delta + m\pi/4)]$$
$$- 2a^2\cos^2(\arg\delta + m\pi/4)\cos[2ay\cos(\arg\delta + m\pi/4)]\}$$
$$= \sum_{m=0}^{1}\{-a^2[1 - \cos 2(\arg\delta + m\pi/4)]\cos[2ay\sin(\arg\delta + m\pi/4)]$$
$$- a^2[1 + \cos 2(\arg\delta + m\pi/4)]\cos[2ay\cos(\arg\delta + m\pi/4)]\}$$
$$= \sum_{m=0}^{1}-[a^2\{\cos[2ay\sin(\arg\delta + m\pi/4)] + \cos[2ay\cos(\arg\delta + m\pi/4)]\}$$
$$+ a^2\cos 2(\arg\delta + m\pi/4)(\cos[2ay\sin(\arg\delta + m\pi/4)] - \cos(2ay\cos[\arg\delta + m\pi/4)])\}. \tag{D5}$$

Further simplifying with the help of Eq. (D4), we obtain

$$
\cos[2ay\sin{(\arg\delta + {}^{m\pi}/4)}] + \cos[2ay\cos{(\arg\delta + {}^{m\pi}/4)}] = 2J_0(2ay) + 4\sum_{s=1}^{\infty}J_{4s}(2ay)\cos[4s(\arg\delta + {}^{m\pi}/4)] \tag{D6}
$$

and

$$
\cos[2ay\sin{(\arg\delta + {}^{m\pi}/4)}] - \cos[2ay\cos{(\arg\delta + {}^{m\pi}/4)}] = 4\sum_{s=1}^{\infty}J_{4s-2}(2ay)\cos[(4s-2)(\arg\delta + {}^{m\pi}/4)]. \tag{D7}
$$

Inserting these back in Eq. (D5) in yields

$$
A_2(y; a, \arg\delta) = 4a^2 J_2(2ay) - 4a^2 J_0(2ay) + \sum_{m=0}^{1}\sum_{s=1}^{\infty}[(2J_{4s-2}(2ay) + 2J_{4s+2}(2ay) - 4J_{4s}(2ay))a^2\cos(4s(\arg\delta + {}^{2\pi ms}/2))]
$$

$$
= 4a^2 J_2(2ay) - 4a^2 J_0(2ay) + 2a^2[2J_6(2ay) + 2J_{10}(2ay) - 4J_8(2ay)]\cos{(8\arg\delta)}. \tag{D8}
$$

Similarly, we can find B_2 and C_2 by substituting the relevant Jacobi-Anger expressions in Eqs. (D2), (D3), and simplifying as shown for A_2.

APPENDIX E: DETAILS OF TAYLOR SERIES EXPANSION FOR THE SUPERPOSITION OF n COMPASS STATES

For the superposition of an arbitrary number n of compass states, the overlap (54) vanishes when

$$
\sum_{m=0}^{n-1}\{\cos[2a|\delta|\cos{(\arg\delta + {}^{m\pi}/2n)}] + \cos[2a|\delta|\sin{(\arg\delta + {}^{m\pi}/2n)}]\} \equiv 0. \tag{E1}
$$

To obtain approximate solutions, we assign the direction of phase-space displacement as $\arg\delta$ and assign the size a pertaining to both compass states in the superposition. We then calculate the Taylor series for Eq. (E1) around some $y \in \mathbb{R}$. We truncate the Taylor series to quadratic order. The Taylor series of the first term in Eq. (E1) is

$$
\cos[2a|\delta|\cos{(\arg\delta + {}^{m\pi}/2n)}] = \cos[2ay\cos{(\arg\delta + {}^{m\pi}/2n)}] - \sin[2ay\cos{(\arg\delta + {}^{m\pi}/2n)}]2a\cos{(\arg\delta + {}^{m\pi}/2n)}(|\delta| - y)
$$

$$
- \cos[2ay\cos{(\arg\delta + {}^{m\pi}/2n)}]2a^2\cos^2{(\arg\delta + {}^{m\pi}/2n)}(|\delta| - y)^2 \tag{E2}
$$

and the Taylor series of the second term in Eq. (E1) is

$$
\cos[2a|\delta|\sin{(\arg\delta + {}^{m\pi}/2n)}] = \cos[2ay\sin{(\arg\delta + {}^{m\pi}/2n)}] - \sin[2ay\sin{(\arg\delta + {}^{m\pi}/2n)}]2a\sin{(\arg\delta + {}^{m\pi}/2n)}(|\delta| - y)
$$

$$
- \cos[2ay\sin{(\arg\delta + {}^{m\pi}/2n)}]2a^2\sin^2{(\arg\delta + {}^{m\pi}/2n)}(|\delta| - y)^2. \tag{E3}
$$

The Taylor series of Eq. (E1) is the sum of both these series.

APPENDIX F: FORM OF QUADRATIC COEFFICIENTS FOR SUPERPOSITION OF n COMPASS STATES

The coefficients of the quadratic equation $[A_n(|\delta|)^2 + B_n(|\delta|) + C_n]$ for a fixed $\arg\delta$ and a for the region $||\delta| - y| \ll 1$ are

$$
A_n(y; a, \arg\delta) = \sum_{m=0}^{n-1}\{-2a^2\sin^2{(\arg\delta + {}^{m\pi}/2n)}\cos[2ay\sin{(\arg\delta + {}^{m\pi}/2n)}]
$$

$$
- 2a^2\cos^2{(\arg\delta + {}^{m\pi}/2n)}\cos[2ay\cos{(\arg\delta + {}^{m\pi}/2n)}]\} \tag{F1}
$$

for the quadratic term,

$$
B_n(y; a, \arg\delta) = \sum_{m=0}^{n-1}\{4a^2 y\sin^2{(\arg\delta + {}^{m\pi}/2n)}\cos[2ay\sin{(\arg\delta + {}^{m\pi}/2n)}] - 2a\sin{(\arg\delta + {}^{m\pi}/2n)}\sin[2ay\sin{(\arg\delta + {}^{m\pi}/2n)}]
$$

$$
+ 4a^2 y\cos^2{(\arg\delta + {}^{m\pi}/2n)}\cos[2ay\cos{(\arg\delta + {}^{m\pi}/2n)}] - 2a\cos{(\arg\delta + {}^{m\pi}/2n)}\sin[2ay\cos{(\arg\delta + {}^{m\pi}/2n)}]\} \tag{F2}
$$

for the linear term, and

$$
C_n(y; a, \arg\delta) = \sum_{m=0}^{n-1}\{2ay\sin{(\arg\delta + {}^{m\pi}/2n)}\sin[2ay\sin{(\arg\delta + {}^{m\pi}/2n)}] - 2a^2 y^2\sin^2{(\arg\delta + {}^{m\pi}/2n)}\cos[2ay\sin{(\arg\delta + {}^{m\pi}/2n)}]
$$

$$
+ \cos[2ay\sin{(\arg\delta + {}^{m\pi}/2n)}] + \cos[2ay\cos{(\arg\delta + {}^{m\pi}/2n)}] + 2ay\cos{(\arg\delta + {}^{m\pi}/2n)}
$$

$$
\times \sin[2ay\cos{(\arg\delta + {}^{m\pi}/2n)}] - 2a^2 y^2\cos^2{(\arg\delta + {}^{m\pi}/2n)}\cos[2ay\cos{(\arg\delta + {}^{m\pi}/2n)}]\}. \tag{F3}
$$

for the constant. We further simplify Eq. (F1) to

$$
\begin{aligned}
A_n(y; a, \arg \delta) &= \sum_{m=0}^{n-1} \{ -2a^2 \sin^2(\arg \delta + {}^{m\pi}/_{2n}) \cos[2ay \sin(\arg \delta + {}^{m\pi}/_{2n})] \\
&\quad - 2a^2 \cos^2(\arg \delta + {}^{m\pi}/_{2n}) \cos[2ay \cos(\arg \delta + {}^{m\pi}/_{2n})] \} \\
&= \sum_{m=0}^{n-1} \{ -a^2[1 - \cos 2(\arg \delta + {}^{m\pi}/_{2n})] \cos[2ay \sin(\arg \delta + {}^{m\pi}/_{2n})] \\
&\quad - a^2[1 + \cos 2(\arg \delta + {}^{m\pi}/_{2n})] \cos[2ay \cos(\arg \delta + {}^{m\pi}/_{2n})] \} \\
&= \sum_{m=0}^{n-1} -[a^2(\cos[2ay \sin(\arg \delta + {}^{m\pi}/_{2n})] + \cos[2ay \cos(\arg \delta + {}^{m\pi}/_{2n})]) \\
&\quad + a^2 \cos 2(\arg \delta + {}^{m\pi}/_{2n})(\cos[2ay \sin(\arg \delta + {}^{m\pi}/_{2n})] - \cos(2ay \cos[\arg \delta + {}^{m\pi}/_{2n})])].
\end{aligned}
\tag{F4}
$$

Further simplifying with the help of Eq. (D4) we obtain

$$
\cos[2ay \sin(\arg \delta + {}^{m\pi}/_{2n})] + \cos[2ay \cos(\arg \delta + {}^{m\pi}/_{2n})] = 2J_0(2ay) + 4\sum_{s=1}^{\infty} J_{4s}(2ay) \cos[4s(\arg \delta + {}^{m\pi}/_{2n})]
\tag{F5}
$$

and

$$
\cos[2ay \sin(\arg \delta + {}^{m\pi}/_{2n})] - \cos[2ay \cos(\arg \delta + {}^{m\pi}/_{2n})] = 4\sum_{s=1}^{\infty} J_{4s-2}(2ay) \cos[(4s-2)(\arg \delta + {}^{m\pi}/_{2n})].
\tag{F6}
$$

Inserting these back in Eq. (F4) yields

$$
\begin{aligned}
A_n(y; a, \arg \delta &= 2a^2 n J_2(2ay) - 2a^2 n J_0(2ay) + \sum_{m=0}^{n-1} \sum_{s=1}^{\infty} [(2J_{4s-2}(2ay) + 2J_{4s+2}(2ay) - 4J_{4s}(2ay))a^2 \cos(4s(\arg \delta + {}^{2\pi ms}/_n))] \\
&= 2a^2 n J_2(2ay) - 2a^2 n J_0(2ay) + na^2(2J_{4n-2}(2ay) + 2J_{4n+2}(2ay) - 4J_{4n}(2ay)) \cos(4n(\arg \delta)).
\end{aligned}
\tag{F7}
$$

Similarly, we can find B_n and C_c by substituting the relevant Jacobi-Anger expressions in Eqs. (F2), (F3), and simplifying as shown for A_n.

[1] E. Schrödinger, Die gegenwärtige Situation in der Quanten-mechanik, Naturwissenschaften **23**, 807 (1935).

[2] R. J. Glauber, Coherent and incoherent states of the radiation field, Phys. Rev. **131**, 2766 (1963).

[3] V. Bužek, A. Vidiella-Barranco, and P. L. Knight, Superpositions of coherent states: Squeezing and dissipation, Phys. Rev. A **45**, 6570 (1992).

[4] V. V. Dodonov, I. A. Malkin, and V. I. Man'ko, Even and odd coherent states and excitations of a singular oscillator, Physica **72**, 597 (1974).

[5] W. H. Zurek, Sub-plank structure in phase space and its relevance for quantum decoherence, Nature (London) **412**, 712 (2001).

[6] A. Kumari, A. K. Pan, and P. K. Panigrahi, Sub-Planck structure in a mixed state, Eur. Phys. J. D **69**, 248 (2015).

[7] F. Toscano, D. A. R. Dalvit, L. Davidovich, and W. H. Zurek, Sub-Planck phase-space structures and Heisenberg-limited measurements, Phys. Rev. A **73**, 023803 (2006).

[8] D. A. R. Dalvit, R. L. de Matos Filho, and F. Toscano, Quantum metrology at the Heisenberg limit with ion trap motional compass states, New J. Phys. **8**, 276 (2006).

[9] W. P. Schleich, *Quantum Optics in Phase Space* (Wiley-VCH, Weinheim, Germany, 2001).

[10] G. S. Agarwal and P. K. Pathak, Mesoscopic superposition of states with sub-Planck structures in phase space, Phys. Rev. A **70**, 053813 (2004).

[11] P. K. Pathak and G. S. Agarwal, Generation of a superposition of multiple mesoscopic states of radiation in a resonant cavity, Phys. Rev. A **71**, 043823 (2005).

[12] N. Akhtar, B. C. Sanders, and C. Navarrete-Benlloch, Sub-Planck structures: Analogies between the Heisenberg-Weyl and SU(2) groups, Phys. Rev. A **103**, 053711 (2021).

[13] N. Akhtar, B. C. Sanders, and G. Xianlong, Sub-Planck phase-space structure and sensitivity for SU(1,1) compass states, Phys. Rev. A **106**, 043704 (2022).

[14] L. Praxmeyer, C.-C. Chen, P. Yang, S.-D. Yang, and R.-K. Lee, Direct measurement of time-frequency analogs of sub-Planck structures, Phys. Rev. A **93**, 053835 (2016).

[15] B. Vlastakis, G. Kirchmair, Z. Leghtas, S. E. Nigg, L. Frunzio, S. M. Girvin, M. Mirrahimi, M. H. Devoret, and R. J. Schoelkopf, Deterministically encoding quantum information using 100-photon schrödinger cat states, Science **342**, 607 (2013).

[16] N. Ofek, A. Petrenko, R. Heeres, P. Reinhold, Z. Leghtas, B. Vlastakis, Y. Liu, L. Frunzio, S. M. Girvin, L. Jiang, M. Mirrahimi, M. H. Devoret, and R. J. Schoelkopf, Extending the lifetime of a quantum bit with error correction in superconducting circuits, Nature (London) **536**, 441 (2016).

[17] G. B. Lemos, R. M. Gomes, S. P. Walborn, P. H. Souto Ribeiro, and F. Toscano, Experimental observation of quantum chaos in a beam of light, Nat. Commun. **3**, 1211 (2012).

[18] D. R. Austin, T. Witting, A. S. Wyatt, and I. A. Walmsley, Measuring sub-Planck structural analogues in chronocyclic phase space, Opt. Commun. **283**, 855 (2010).

[19] P. Jacquod, I. Adagideli, and C. W. J. Beenakker, Decay of the loschmidt echo for quantum states with sub-planck-scale structures, Phys. Rev. Lett. **89**, 154103 (2002).

[20] D. A. Wisniacki, Short-time decay of the Loschmidt echo, Phys. Rev. E **67**, 016205 (2003).

[21] S. Ghosh, A. Chiruvelli, J. Banerji, and P. K. Panigrahi, Mesoscopic superposition and sub-Planck-scale structure in molecular wave packets, Phys. Rev. A **73**, 013411 (2006).

[22] L. Praxmeyer, P. Wasylczyk, C. Radzewicz, and K. Wódkiewicz, Time-frequency domain analogues of phase space sub-planck structures, Phys. Rev. Lett. **98**, 063901 (2007).

[23] A. J. Scott and C. M. Caves, Teleportation fidelity as a probe of sub-Planck phase-space structure, Ann. Phys. (NY) **323**, 2685 (2008).

[24] J. R. Bhatt, P. K. Panigrahi, and M. Vyas, Entanglement-induced sub-Planck phase-space structures, Phys. Rev. A **78**, 034101 (2008).

[25] M. Stobińska, G. J. Milburn, and K. Wódkiewicz, Wigner function evolution of quantum states in the presence of self-Kerr interaction, Phys. Rev. A **78**, 013810 (2008).

[26] S. Ghosh, U. Roy, C. Genes, and D. Vitali, Sub-Planck-scale structures in a vibrating molecule in the presence of decoherence, Phys. Rev. A **79**, 052104 (2009).

[27] U. Roy, S. Ghosh, P. K. Panigrahi, and D. Vitali, Sub-Planck-scale structures in the Pöschl-Teller potential and their sensitivity to perturbations, Phys. Rev. A **80**, 052115 (2009).

[28] V. V. Dodonov, C. Valverde, L. S. Souza, and B. Baseia, Decoherence of odd compass states in the phase-sensitive amplifying/dissipating environment, Ann. Phys. (NY) **371**, 296 (2016).

[29] P. Kumar and R.-K. Lee, Sensitivity of sub-planck structures of mesoscopically superposed coherent states to the thermal reservoirs induced decoherence, Opt. Commun. **394**, 23 (2017).

[30] L. A. Howard, T. J. Weinhold, F. Shahandeh, J. Combes, M. R. Vanner, A. G. White, and M. Ringbauer, Quantum hypercube states, Phys. Rev. Lett. **123**, 020402 (2019).

[31] J. Janszky, P. Domokos, and P. Adam, Coherent states on a circle and quantum interference, Phys. Rev. A **48**, 2213 (1993).

[32] J.-P. Gazeau, *Coherent States in Quantum Physics* (Wiley-VCH, Weinheim, Germany, 2009).

[33] P. Domokos, P. Adam, and J. Janszky, One-dimensional coherent-state representation on a circle in phase space, Phys. Rev. A **50**, 4293 (1994).

[34] C. Navarrete-Benlloch, *An Introduction to the Formalism of Quantum Information with Continuous Variables* (Morgan and Claypool/IOP, Bristol, England, 2015), pp. 2053–2571.

[35] D. V. Sychev, A. E. Ulanov, A. A. Pushkina, M. W. Richards, I. A. Fedorov, and A. I. Lvovsky, Enlargement of optical schrödinger's cat states, Nat. Photonics **11**, 379 (2017).